

Comparative Study of Solar Radiation Models for the Estimation of Solar Radiation Using Short-Term Meteorological Data in Lawra, Ghana

Emmanuel A. Sarsah, Adams Yunus, Abdul-Rahim Bawa, and Joshua A. Akanbasiam

Abstract — Monthly average daily global solar radiation data are essential for the design and study of solar energy systems. The performance and accuracy of eleven models for the estimation of monthly average global solar radiation were compared in this study. Nineteen months (Nov 2020 – May 2022) ground measurement data consisting of monthly mean daily sunshine duration, relative humidity, minimum and maximum temperatures, and global solar radiation collected from the Lawra Solar Plant were used. The models were compared using statistical indices. According to the indices, most of the models were in reasonably good agreement with the measured data. Two model equations, however, were found to have the highest accuracy and can thus be used to estimate monthly average global solar radiation in Lawra and other places with similar climatic conditions where radiation data is unavailable.

Keywords — Estimation, Models, Solar Radiation, Sunshine Hours.

I. INTRODUCTION

Most solar energy applications, such as solar energy system simulation, require at the very least knowledge of daily values of global solar radiation on a horizontal surface. Thus, accurate estimation of daily values of global radiation data is essential for the design and long-term evaluation in applications such as meteorological forecasting, solar heating, drying, air-conditioning, and architectural design. The most important parameters that are frequently required in the solar energy applications listed above are the average solar irradiation and its components; measurements of which are not available at every location, particularly in developing countries, due to the cost, maintenance, and calibration requirements of the measuring equipment.

As a result, many empirical models have been developed that can be used to estimate global solar radiation using more readily available meteorological parameters such as sunshine hours, relative humidity, and ambient temperature. Empirical modeling is an important and cost-effective tool for estimating global solar radiation. The accuracy of such models is determined by the quality of the measured data. Though less accurate, modeling is a better tool for estimating global solar radiation in areas where measurements are unavailable [1]. Angstrom [2] created the first model for estimating global radiation in 1924, which used sunshine

hours and clear sky radiation data. Prescott [3] modified the Angstrom relation in 1940 in order to resolve the ambiguity in the definition of clear sky global solar radiation.

Many such models have since been developed and tested by researchers all over the world [4]. Numerous studies have been conducted on the relationship between global radiation and sunshine duration, for which data from an increasing number of meteorological stations are now available [5]-[9]. Other empirical models have been developed to calculate solar radiation from other parameters such as relative humidity and ambient temperature [4]. In 1994, Garcia [4] proposed a model for estimating global solar radiation based on sunshine hours and temperature.

Sarsah and Uba [1] investigated the relationship between global solar radiation and factors such as relative humidity, sunshine duration, and solar declination. A multilinear two-parameter regression model was developed in Nigeria to estimate global solar radiation [4]. The authors combined the Garcia model with the Angstrom-Prescott model to develop a new model with three regression constants.

Long-term average daily radiation data are typically used in all of the models reviewed. However, for locations where such long-term data is not available, such as most of Ghana, it would be interesting to investigate how the models will perform on short-term data. Thus, the aim of the current study was to compare solar radiation models whose parameters were measured at the Lawra Solar Power Plant (LSPP) in Ghana's Upper West region, and to select the model with the highest accuracy.

II. METHODOLOGY

A. Theory

Prescott modified Angstrom's model and developed (1) for estimating global solar radiation.

$$\frac{\bar{H}}{\bar{H}_0} = a + b \left(\frac{\bar{n}}{\bar{N}} \right) \quad (1)$$

where \bar{H} is the monthly mean daily global solar radiation ($\text{MJ}/\text{m}^2 \text{ day}$), \bar{H}_0 is the monthly average daily extraterrestrial radiation ($\text{MJ}/\text{m}^2 \text{ day}$), \bar{n} is the monthly average daily sunshine hours (hr), \bar{N} is the monthly average maximum daily

Submitted on December 30, 2022.

Published on March 02, 2023.

E. A. Sarsah, Dr. Hilla Limann Technical University, Ghana.

(e-mail: emmanuel.sarsah@dhltu.edu.gh)

A. Yunus, Dr. Hilla Limann Technical University, Ghana.

(e-mail: dms_yunus@yahoo.com)

A.-R. Bawa, Dr. Hilla Limann Technical University, Ghana.

(e-mail: kascowemah@yahoo.com)

J. A. Akanbasiam, Dr. Hilla Limann Technical University, Ghana.

(e-mail: ja.akanbasiam@gmail.com)

hours of sunshine (hr), a and b are empirical constants.

Other models for estimating \bar{H} have been developed by different authors and are in (2) to (11), which we will sometimes refer to as model equations.

$$\frac{\bar{H}}{\bar{H}_0} = a + b \left(\frac{\bar{n}}{\bar{N}}\right) + c \left(\frac{\bar{n}}{\bar{N}}\right)^2 \quad (\text{Akinoglu and Ecevit [10]}) \quad (2)$$

$$\frac{\bar{H}}{\bar{H}_0} = a + b \left(\frac{\bar{n}}{\bar{N}}\right) + c \left(\frac{\bar{n}}{\bar{N}}\right)^2 + d \left(\frac{\bar{n}}{\bar{N}}\right)^3 \quad (\text{Samuel [11]}) \quad (3)$$

$$\frac{\bar{H}}{\bar{H}_0} = a + b \left(\frac{\bar{n}}{\bar{N}}\right) + c \log\left(\frac{\bar{n}}{\bar{N}}\right) \quad (\text{Newland [12]}) \quad (4)$$

$$\frac{\bar{H}}{\bar{H}_0} = a + b \log\left(\frac{\bar{n}}{\bar{N}}\right) \quad (\text{Ampratwum [13]}) \quad (5)$$

$$\frac{\bar{H}}{\bar{H}_0} = a + b \left(\frac{\bar{n}}{\bar{N}}\right) + c \exp\left(\frac{\bar{n}}{\bar{N}}\right) \quad (\text{Bakirci [14]}) \quad (6)$$

$$\frac{\bar{H}}{\bar{H}_0} = a + b \exp\left(\frac{\bar{n}}{\bar{N}}\right) \quad (\text{Almorox, Benito and Hontoria [15]}) \quad (7)$$

$$\frac{\bar{H}}{\bar{H}_0} = a \left(\frac{\bar{n}}{\bar{N}}\right)^b \quad (\text{Bakirci [14]}) \quad (8)$$

$$\frac{\bar{H}}{\bar{H}_0} = a + b \left(\frac{\Delta T}{\bar{N}}\right) \quad (\text{Garcia [4]}) \quad (9)$$

$$\frac{\bar{H}}{\bar{H}_0} = a + b \left(\frac{\bar{n}}{\bar{N}}\right) + c \left(\frac{\Delta T}{\bar{N}}\right) \quad (\text{Olomiyesan and Oyedum [4]}) \quad (10)$$

$$\frac{\bar{H}}{\bar{H}_0} = aT^b\bar{H}_0 + c \quad (\text{Hassan et al. [16]}) \quad (11)$$

where T is the monthly average of daily ambient temperature ($^{\circ}\text{C}$), ΔT is temperature difference = $T_{\max} - T_{\min}$. \bar{N} is obtained from the daylength (N) equation given by (12).

$$N = \frac{2}{15} \cos^{-1}[-\tan(L) \tan(\delta)] \quad (12)$$

where L = local latitude and δ = declination, in degrees. For any day of the year, d , the declination can be found by using (13) where $1 \leq d \leq 365$.

$$\delta = 23.45 \sin\left[\frac{360}{365}(284 + d)\right] \quad (13)$$

\bar{H}_0 is calculated from the total radiation H_0 incident on an extraterrestrial horizontal surface using (14).

$$H_0 = \frac{24 \times 3600 \times G_{sc}}{\pi} \left[1 + 0.033 \cos\left(\frac{360N}{365}\right) \times \left[\cos(L) \cos(\delta) \sin(h_{ss}) + \left(\frac{\pi h_{ss}}{180}\right) \sin(L) \sin(\delta) \right] \right] \quad (14)$$

where G_{sc} = solar constant = 1366.1 W/m^2 , h_{ss} = sunset hour angle, in degrees, obtained using (15).

$$h_{ss} = \cos^{-1}[\tan(L) \tan(\delta)] \quad (15)$$

\bar{H}_0 is then calculated from (14) by choosing a particular day of the year in the given month for which the daily total extraterrestrial radiation is estimated to be the same as the

monthly mean value [17]. However, it can also be obtained from Table I.

B. Statistical Analysis

Statistical indicators in (16) to (18) were used to test the accuracy of the eleven model equations presented. The indicators include mean bias error (MBE), mean percentage error (MPE), root mean square error (RMSE) and the coefficient of determination R^2 .

$$MBE = \frac{1}{n} \sum_{i=1}^n (\bar{H}_{i,c} - \bar{H}_{i,m}) \quad (16)$$

Where $\bar{H}_{i,c}$ and $\bar{H}_{i,m}$ are the calculated and measured values of \bar{H} and n is the number of observations. A low MBE value is desired.

$$MPE(\%) = \frac{100}{n} \sum_{i=1}^n \left(\frac{\bar{H}_{i,c} - \bar{H}_{i,m}}{\bar{H}_{i,m}} \right) \quad (17)$$

MPE between -10% and +10% is considered acceptable.

$$RMSE = \sqrt{\frac{1}{n} \sum_{i=1}^n (\bar{H}_{i,c} - \bar{H}_{i,m})^2} \quad (18)$$

The smaller the value of RMSE, the better is the model's performance.

$$R^2 = 1 - \frac{\sum_{i=1}^n (\bar{H}_{i,m} - \bar{H}_{i,c})^2}{\sum_{i=1}^n (\bar{H}_{i,m} - \bar{H}_m)^2} \quad (19)$$

where \bar{H}_m is the average value of the measured and calculated values. R^2 gives information about the goodness of fit of a model and explains the percentage of the variability in the response variable as explained by the variation in the predictor variable.

C. Study Site

The data for the study was obtained from the Volta River Authority's (VRA) LSPP in Ghana. VRA is Ghana's primary power generation authority, responsible for generating, transmitting and distributing electricity. It is owned by the Government of Ghana. Lawra is located at 10.6N , 2.8W and has an elevation of 283 m above sea level. The LSPP has an installation capacity of 6.5 MWp and a land area of approximately 6.13 ha, supplying electricity to approximately 15,000 households [18]. The data was recorded in 5 minutes interval from November 2020 to May 2022. For 2020, we obtained data for the months November and December whereas the 2022 data was from January to May. Only for the year 2021 was complete data from January to December available. The horizontal irradiance was recorded in W/m^2 .

D. Method

In order to get the monthly averages of the measured radiation data obtained, we used the pivot table functionality in the Spreadsheet application of the WPS Office software. Using the conversion factor of $1 \text{ W/m}^2 = 0.086 \text{ MJ/m}^2$, we converted the values from W/m^2 to MJ/m^2 .

TABLE I: MONTHLY AVERAGE DAILY EXTRATERRESTRIAL INSOLATION ON HORIZONTAL SURFACE (MJ/M² DAY) [17]

| Latitude | Jan 17 | Feb 16 | Mar 16 | Apr 15 | May 15 | Jun 11 | Jul 17 | Aug 16 | Sep 15 | Oct 15 | Nov 14 | Dec 10 |
|----------|--------|--------|--------|--------|--------|--------|--------|--------|--------|--------|--------|--------|
| 60 °S | 41.1 | 31.9 | 21.2 | 10.9 | 4.4 | 2.1 | 3.1 | 7.8 | 16.7 | 28.1 | 38.4 | 43.6 |
| 55 °S | 41.7 | 33.7 | 23.8 | 13.8 | 7.1 | 4.5 | 5.6 | 10.7 | 19.5 | 30.2 | 39.4 | 43.9 |
| 50 °S | 42.4 | 35.3 | 26.3 | 16.8 | 10 | 7.2 | 8.4 | 13.6 | 22.2 | 32.1 | 40.3 | 44.2 |
| 45 °S | 42.9 | 36.8 | 28.6 | 19.6 | 12.9 | 10 | 11.2 | 16.5 | 24.7 | 33.8 | 41.1 | 44.4 |
| 40 °S | 43.1 | 37.9 | 30.7 | 22.3 | 15.8 | 12.9 | 14.1 | 19.3 | 27.1 | 35.3 | 41.6 | 44.4 |
| 35 °S | 43.2 | 38.8 | 32.5 | 24.8 | 18.6 | 15.8 | 17 | 22 | 29.2 | 36.5 | 41.9 | 44.2 |
| 30 °S | 43 | 39.5 | 34.1 | 27.2 | 21.4 | 18.7 | 19.8 | 24.5 | 31.1 | 37.5 | 41.9 | 43.7 |
| 25 °S | 42.5 | 39.9 | 35.4 | 29.4 | 24.1 | 21.5 | 22.5 | 26.9 | 32.8 | 38.1 | 41.6 | 43 |
| 20 °S | 41.5 | 39.9 | 36.5 | 31.3 | 26.6 | 24.2 | 25.1 | 29.1 | 34.2 | 38.5 | 41.1 | 42 |
| 15 °S | 40.8 | 39.7 | 37.2 | 33.1 | 28.9 | 26.8 | 27.6 | 31.1 | 35.4 | 38.7 | 40.3 | 40.8 |
| 10 °S | 39.5 | 39.3 | 37.7 | 34.6 | 31.1 | 29.2 | 29.9 | 32.8 | 36.3 | 38.5 | 39.3 | 39.3 |
| 5 °S | 38 | 38.5 | 38 | 35.8 | 33 | 31.4 | 32 | 34.4 | 36.9 | 38.1 | 37.9 | 37.6 |
| 0 | 36.2 | 37.4 | 37.9 | 36.8 | 34.8 | 33.5 | 33.9 | 35.7 | 37.2 | 37.3 | 36.4 | 35.6 |
| 5 °N | 34.2 | 36.1 | 37.5 | 37.5 | 36.3 | 35.3 | 35.6 | 36.7 | 37.3 | 36.3 | 34.5 | 33.5 |
| 10 °N | 32 | 34.6 | 36.9 | 37.9 | 37.5 | 37 | 37.1 | 37.5 | 37 | 35.1 | 32.5 | 31.1 |
| 15 °N | 29.5 | 32.7 | 35.9 | 38 | 38.5 | 38.4 | 38.3 | 38 | 36.5 | 33.5 | 30.2 | 28.5 |
| 20 °N | 26.9 | 30.7 | 34.7 | 37.9 | 39.3 | 39.5 | 39.3 | 38.2 | 35.7 | 31.8 | 27.7 | 25.7 |
| 25 °N | 24.1 | 28.4 | 33.3 | 37.5 | 39.8 | 40.4 | 40 | 38.2 | 34.7 | 29.8 | 25.1 | 22.9 |
| 30 °N | 21.3 | 26 | 31.6 | 36.8 | 40 | 41.1 | 40.4 | 37.9 | 33.4 | 27.5 | 22.3 | 19.9 |
| 35 °N | 18.3 | 23.3 | 29.6 | 35.8 | 39.9 | 41.5 | 40.6 | 37.3 | 31.8 | 25.1 | 19.4 | 16.8 |
| 40 °N | 15.2 | 20.5 | 27.4 | 34.6 | 39.7 | 41.7 | 40.6 | 36.5 | 30 | 22.5 | 16.4 | 13.7 |
| 45 °N | 12.1 | 17.6 | 25 | 33.1 | 39.2 | 41.7 | 40.4 | 35.4 | 27.9 | 19.8 | 13.4 | 10.7 |
| 50 °N | 9.1 | 14.6 | 22.5 | 31.4 | 38.4 | 41.5 | 40 | 34.1 | 25.7 | 16.9 | 10.4 | 7.7 |
| 55 °N | 6.1 | 11.6 | 19.7 | 29.5 | 37.6 | 41.3 | 39.4 | 32.7 | 23.2 | 13.9 | 7.4 | 4.8 |
| 60 °N | 3.4 | 8.5 | 16.8 | 27.4 | 36.6 | 41 | 38.8 | 31 | 20.6 | 10.9 | 4.5 | 2.3 |

Also, the average temperature, the minimum and maximum temperatures for each month were obtained using the pivot table tool. ΔT was then found using the relation $\Delta T = T_{max} - T_{min}$ for each month.

For the \bar{H}_o values, we performed linear interpolation using the latitude of Lawra between 10°N and 15°N from Table I. Similarly, to find \bar{N} , (12) was used with the average day of each month obtained from Table I. The ratio $\Delta T/\bar{N}$ was then computed for each month. For the ratio \bar{n}/\bar{N} , we used data at Wa in the work by Sarsah and Uba [1] because the Lawra data we got did not record daily hours of sunshine. The geographical location of Wa is 10.06°N, 2.5W with an altitude of 322 m above sea level and has weather conditions similar to Lawra.

To obtain the constants a , b , c and d from the model equations, the *fit regression model* tool in the Minitab software package was used. The constants were substituted in their respective model equations. The model equations were then used to estimate \bar{H} for each month and compared with the measured ones using the statistical tests.

III. RESULTS AND DISCUSSION

The summary of the data obtained from Section D is in Table II. The regression coefficients are in Table III. In Table IV are the estimated values of \bar{H} using the regression models whereas the statistical error tests of the models are in Table V. The MBEs of the models were all low ranging from 0.047 for (2) to -0.647 for (6) implying that (2) performed best whereas (6) had the worst score. The ranking of the models in order of low MBEs is as in Fig. 1.

The MPE of all models were in the acceptable range of -10% to +10%. However, (2) performed best with an MPE of 0.737% whereas (6) was the worst model with a value of -3.105%. The performance of the models in order of low MPEs is as in Fig. 2.

For the RMSE test, (11) had the lowest value of 0.987 whereas (9) had the highest value. The RMSE ranking from the best model to the worst model is as in Fig. 3. The R^2 values of all models were reasonably good except for (9), with (11) being the best. The R^2 test is as in Fig. 4.

TABLE II: SUMMARY

| Month | \bar{H} (MJ/m ² day) | \bar{H}_o (MJ/m ² day) | T_{max} (°C) | T_{min} (°C) | ΔT | T (°C) | \bar{H}/\bar{H}_o | \bar{n}/\bar{N} | $\Delta T/\bar{N}$ |
|-----------|--------------------------------------|--|----------------|----------------|------------|----------|---------------------|-------------------|--------------------|
| January | 20.00 | 31.68 | 38.35 | 13.43 | 24.92 | 26.21 | 0.63 | 0.48 | 2.18 |
| February | 21.95 | 31.76 | 39.80 | 12.52 | 27.28 | 28.55 | 0.69 | 0.48 | 2.34 |
| March | 20.99 | 31.87 | 40.85 | 20.55 | 20.30 | 31.67 | 0.66 | 0.51 | 1.68 |
| April | 21.09 | 32.01 | 41.50 | 19.90 | 21.60 | 31.22 | 0.66 | 0.51 | 1.77 |
| May | 20.42 | 32.13 | 39.40 | 21.70 | 17.70 | 29.98 | 0.64 | 0.49 | 1.42 |
| June | 18.54 | 32.18 | 37.80 | 5.90 | 31.90 | 27.65 | 0.58 | 0.44 | 2.53 |
| July | 16.60 | 32.15 | 33.95 | 20.05 | 13.90 | 26.25 | 0.52 | 0.41 | 1.11 |
| August | 14.38 | 32.06 | 99.82 | 5.90 | 93.92 | 25.06 | 0.45 | 0.37 | 7.61 |
| September | 16.88 | 31.94 | 34.95 | 18.83 | 16.12 | 26.21 | 0.53 | 0.40 | 1.34 |
| October | 19.94 | 31.80 | 37.20 | 21.50 | 15.70 | 27.97 | 0.63 | 0.50 | 1.34 |
| November | 20.79 | 31.71 | 38.45 | 15.02 | 23.43 | 27.47 | 0.66 | 0.43 | 2.04 |
| December | 17.96 | 31.67 | 38.20 | 13.60 | 24.60 | 26.6 | 0.57 | 0.46 | 2.16 |

TABLE III: REGRESSION COEFFICIENTS

| Equation Number | a | b | c | d |
|-----------------|-----------|-----------|----------|----|
| 1 | 0 | 1.317 | - | - |
| 2 | -1.91 | -9.70 | - | - |
| 3 | -6.4 | 41.1 | -81 | 54 |
| 4 | 6.86 | -7.19 | 8.68 | - |
| 5 | 1.067 | 1.358 | - | - |
| 6 | 10.77 | 20.7 | -12.43 | - |
| 7 | -0.722 | 0.838 | - | - |
| 8 | 1.30355 | 0.986166 | - | - |
| 9 | 0.6559 | -0.0237 | - | - |
| 10 | 0.074 | 1.187 | -0.00639 | - |
| 11 | -0.285956 | -0.129564 | 6.53267 | - |

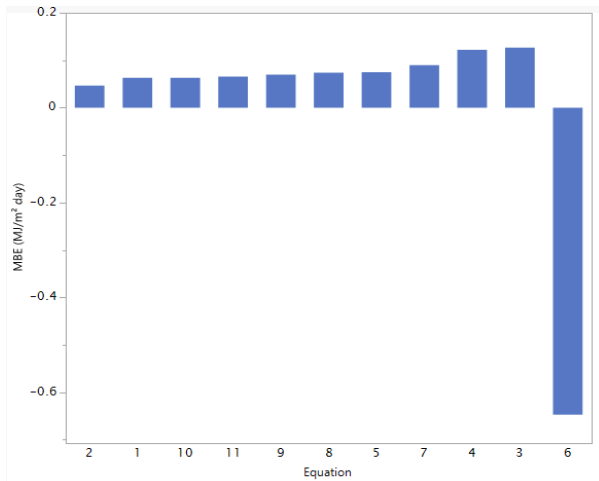


Fig. 1. MBE test.

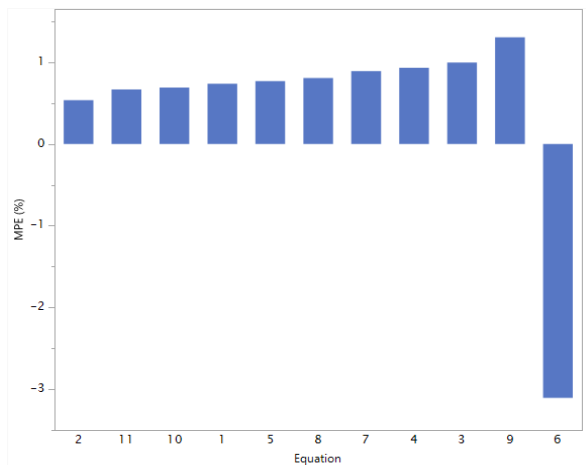


Fig. 2. MPE test.

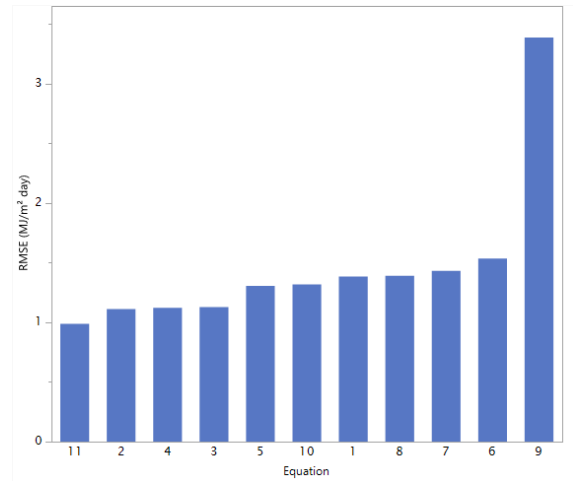


Fig. 3. RMSE test.

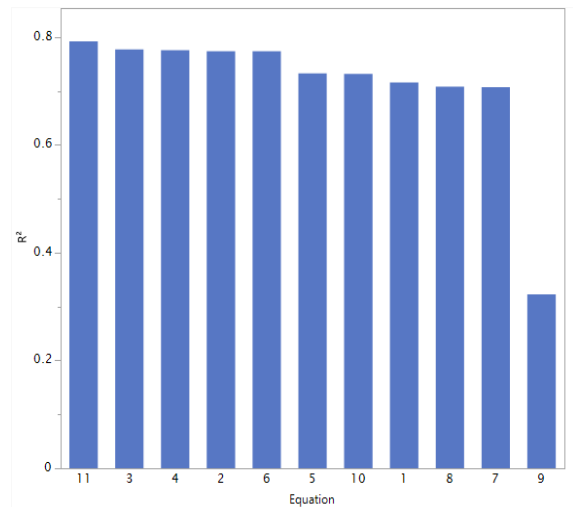


Fig. 4. R^2 test.

From the results of the statistical error analysis, it can be deduced that models (2) and (11) passed all tests and had two scores each as the top performing model in our rankings. This indicates that both models are suitable for estimating \bar{H} in the study site. The two models are as in (20) and (21).

$$\frac{\bar{H}}{\bar{H}_0} = -1.91 + 9.97\left(\frac{\bar{n}}{\bar{N}}\right) - 9.70\left(\frac{\bar{n}}{\bar{N}}\right)^2 \quad (20)$$

$$\frac{\bar{H}}{\bar{H}_0} = -0.285956T^{-0.129564}\bar{H}_0 + 6.53267 \quad (21)$$

The plot of \bar{H} with models (2) and (11) is as in Fig. 5.

TABLE IV: COMPARISON OF MEASURED AND ESTIMATED \bar{H}

| | | Estimated \bar{H} from the model equations | | | | | | | | | | |
|-----------|----------------------|--|-------|-------|-------|-------|-------|-------|-------|-------|-------|-------|
| Month | $\bar{H}_{measured}$ | (1) | (2) | (3) | (4) | (5) | (6) | (7) | (8) | (9) | (10) | (11) |
| January | 20.00 | 20.03 | 20.30 | 20.20 | 20.34 | 20.09 | 19.58 | 20.03 | 20.02 | 19.15 | 19.95 | 18.98 |
| February | 21.95 | 20.08 | 20.35 | 20.25 | 20.39 | 20.14 | 19.63 | 20.08 | 20.08 | 19.07 | 19.97 | 20.64 |
| March | 20.99 | 21.41 | 20.77 | 20.91 | 20.87 | 21.35 | 20.00 | 21.46 | 21.39 | 19.63 | 21.31 | 22.57 |
| April | 21.09 | 21.50 | 20.86 | 21.00 | 20.96 | 21.44 | 20.08 | 21.56 | 21.48 | 19.66 | 21.39 | 21.50 |
| May | 20.42 | 20.73 | 20.77 | 20.69 | 20.81 | 20.77 | 20.03 | 20.75 | 20.73 | 19.99 | 20.77 | 19.88 |
| June | 18.54 | 18.65 | 19.27 | 19.38 | 19.36 | 18.75 | 18.60 | 18.64 | 18.67 | 19.18 | 18.67 | 17.61 |
| July | 16.60 | 17.36 | 17.59 | 17.90 | 17.72 | 17.40 | 16.95 | 17.38 | 17.40 | 20.24 | 17.80 | 16.47 |
| August | 14.38 | 15.62 | 14.46 | 14.53 | 14.48 | 15.41 | 13.90 | 15.75 | 15.68 | 15.25 | 14.89 | 15.81 |
| September | 16.88 | 16.83 | 16.80 | 17.12 | 16.92 | 16.82 | 16.18 | 16.87 | 16.87 | 19.94 | 17.26 | 17.58 |
| October | 19.94 | 20.94 | 20.67 | 20.67 | 20.74 | 20.93 | 19.92 | 20.98 | 20.93 | 19.85 | 20.96 | 19.93 |
| November | 20.79 | 17.96 | 18.51 | 18.69 | 18.61 | 18.05 | 17.85 | 17.95 | 17.98 | 19.27 | 18.12 | 19.97 |
| December | 17.96 | 19.19 | 19.75 | 19.72 | 19.80 | 19.29 | 19.06 | 19.17 | 19.20 | 19.15 | 19.20 | 19.39 |

TABLE V: STATISTICAL MEASURES OF THE MODEL EQUATIONS

| Equation | MBE (MJ/m ² day) | MPE (%) | RMSE (MJ/m ² day) | R ² |
|----------|--------------------------------|---------|---------------------------------|----------------|
| 1 | 0.063 | 0.737 | 1.383 | 0.716 |
| 2 | 0.047 | 0.536 | 1.111 | 0.774 |
| 3 | 0.127 | 0.996 | 1.128 | 0.777 |
| 4 | 0.122 | 0.932 | 1.121 | 0.776 |
| 5 | 0.075 | 0.770 | 1.305 | 0.733 |
| 6 | -0.647 | -3.105 | 1.534 | 0.774 |
| 7 | 0.090 | 0.893 | 1.430 | 0.707 |
| 8 | 0.074 | 0.809 | 1.389 | 0.708 |
| 9 | 0.070 | 1.307 | 3.384 | 0.323 |
| 10 | 0.063 | 0.691 | 1.317 | 0.732 |
| 11 | 0.066 | 0.668 | 0.987 | 0.792 |

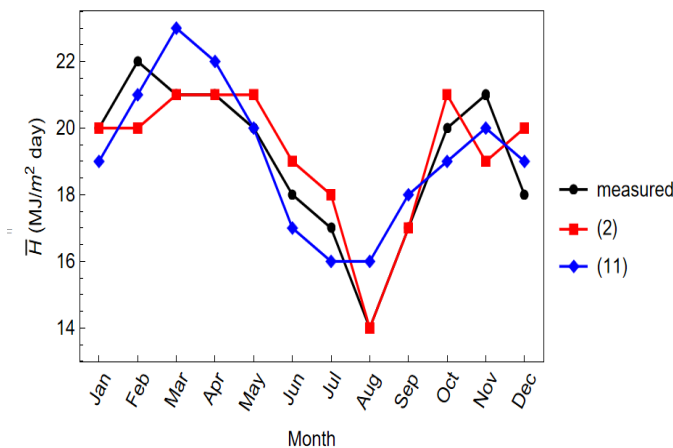


Fig. 5. Comparison of measured and estimated \bar{H} .

IV. CONCLUSION

The objective of this study was to evaluate various solar radiation models for estimation of average daily global solar radiation using short-term ground measurement data and select the most appropriate model. Eleven model equations based on sunshine hours and temperature were selected. The models were compared using the statistical error tests. From the tests, two model equations were selected since they had very similar performance. The two models can be used to estimate \bar{H} at Lawra in the Upper West Region of Ghana and elsewhere with similar climatic conditions where radiation data are unavailable.

ACKNOWLEDGMENT

The authors would like to thank the Deputy Chief Executive Officer of VRA for providing the data used in this study.

CONFLICT OF INTEREST

The authors declare that there is no conflict of interests regarding the publication of this paper.

REFERENCES

- [1] Sarsah EA, Uba FA. Empirical correlations for the estimation of global solar radiation using meteorological data in Wa, Ghana. *Pelagia Research Library*, 2013;4(4):63–71.
- [2] Angstrom A. Solar and terrestrial radiation. Report to the international commission for solar research on actinometric

- investigations of solar and atmospheric radiation. *Quarterly Journal of the Royal Meteorological Society*, 1924 Apr;50(210):121–6.
- [3] Precott JA. Evaporation from water surface in relation to solar radiation. *Transactions of the Royal Society of Australia*, 1940;46:114–8.
- [4] Olomiyesan BM, Oyedum OD. Comparative study of ground measured, satellite-derived, and estimated global solar radiation data in Nigeria. *Journal of Solar Energy*, 2016 Jun 29;2016:1–7.
- [5] Ogbaka DT, Benjamin AH, Jummai VZ. Angstrom-Prescott model for predicting global solar radiation in Mubi, Nigeria. *Asian Journal of Basic Science & Research*, 2020 May 30;2(2):86–92.
- [6] Tsung KY, Tan R, Li GY. Estimating the global solar radiation in putrajaya using the Angstrom-Prescott model. *Earth and Environmental Science*, 2019;268:1–6.
- [7] Djoman MA, Fassinou WF, Memelede A. Calibration of Angstrom-Prescott coefficients to estimate global solar radiation in Côte d'Ivoire. *ESJ Natural/Life/Medical Sciences*, 2021 Oct 31;17(37):24–38.
- [8] Oreshkin B, Hyder MJ, Nauman A, Musheer S. Monthly average solar radiation and angstrom-prescott model for Islamabad, Pakistan. In: *Engineering Proceedings*, 2022: 1–4.
- [9] Ogbaka DT, Nuhu R. Estimation of Global solar radiation using Angstrom type empirical correlation. *IRE Journals*, 2020 Jul;4(1):132–5.
- [10] Akinoglu BG, Ecevit A. Construction of a quadratic model using modified Angstrom coefficients to estimate global solar radiation. *Solar Energy*, 1990;45(2):85–92.
- [11] Samuel TDMA. Estimation of global radiation for Sri Lanka. *Solar Energy*, 1991;47(5):333–7.
- [12] Newland FJ. A study of solar radiation models for the coastal region of South China. *Solar Energy*, 1989;43(4):227–35.
- [13] Ampratwum DB, Dorvlo ASS. Estimation of solar radiation from the number of sunshine hours. *Applied Energy*, 1999 Jul;63(3):161–7.
- [14] Bakirci K. Correlations for estimation of daily global solar radiation with hours of bright sunshine in Turkey. *Energy*, 2009 Apr;34(4):485–501.
- [15] Almorox J, Benito M, Hontoria C. Estimation of monthly Angstrom-Prescott equation coefficients from measured daily data in Toledo, Spain. *Renewable Energy*, 2005 May;30(6):931–6.
- [16] Hassan GE, Youssef ME, Mohamed ZE, Ali MA, Hanafy AA. New temperature-based models for predicting global solar radiation. *Applied Energy*, 2016 Oct;179:437–50.
- [17] Kalogirou SA. *Solar Energy Engineering: Processes and Systems*. Academic Press; 2014.
- [18] Volta River Authority | Lawra Solar Power Plant [Internet]. www.vra.com. [cited 2022 Oct 15]. Available from: https://www.vra.com/our_mandate/lawra_solar_plant.php.